ELSEVIER

Polymer 40 (1999) 3835–3841

polymer

Synthesis and investigation of photoinduced anisotropy of a series of liquid crystalline copolymers with azo groups

Yanqing Tian[a], Jingli Xie[a], Changshun Wang[b], Yingying Zhao[a,*], Haosheng Fei[b]

[a]*Department of Chemistry, Jilin University, Changchun 130023, People's Republic of China*
[b]*Department of Physics, Jilin University, Changchun 130023, People's Republic of China*

Received 16 January 1998; received in revised form 7 July 1998; accepted 4 August 1998

Abstract

A series of liquid-crystalline copolymers poly{6-[4-(4-hexyloxy benzoyloxy)phenoxy]hexyl methacrylate}-co-{6-[4-(*S*-2-methyl-1-butyloxycarbonylphenylazo)phenoxy]hexyl methacrylate} with an azobenzene moiety as photoreactive mesogenic unit were prepared. Their liquid crystalline properties and photoinduced anisotropy were investigated. The results showed that these polymers exhibited layered smectic phases and showed good photoinduced anisotropy both in the glass states and in the mesophase states.

Keywords: Photoinduced anisotropy; Liquid crystalline copolymers; Azo groups

1. Introduction

Side-chain liquid crystalline polymers have caused interest because of their theoretical aspects and potential uses in electro-optical and information-storage devices [1–3]. Particular interest in preparation and investigation of azo-dye containing liquid crystalline polymers has increased recently because of their potential application in optical storage devices due to both the reversibility of the isomerization and the large steric difference between the two isomeric states [4–7]. On the other hand, functional groups such as the azo group, which can be used to study the photoisomerization, and chiral groups can be introduced into polymers easily by the method of copolymerization. Up to now some side chain liquid crystalline chiral copolymers with azo groups have been prepared and investigated [8–11]. For example, Niesel et al. [11] studied poly-{4-ω-methacryloxyhexyloxy-4′-butyloxyazobenzene}-co-{(*S*)-4-(ω-methacryloxyhexyloxy)phenyl-4-(2-methylbutyloxy) benzoate} which showed nematic and metastable S_A phases. Ringsdorf et al. [9] investigated the photoreactive chiral liquid crystalline side-chain azo copolymers poly{4-methyloxyphenyl-4-ω-acryloxyhexyloxybenzoate}-co-poly{4-acryloxyhexyloxy-4′-(*S*-2-methylbutyloxy)azobenzene} which showed cholesteric and smectic phases. In this paper a new series of copolymers with an azobenzene moiety as photoreactive mesogenic unit were prepared and their liquid crystalline behavior was investigated. Polymer **1** (as shown in Fig. 1) was chosen as the achiral example, due to its low glass transition temperature and broad mesophase, and a new polymer **2** as the chiral example containing an azo group, and their photoisomeric properties were studied. These copolymers are analogous but not identical to the copolymers reported in Refs. [9–11].

Because azobenzenes are photochromic and exhibit a light induced *trans–cis* isomerization, so polymers with azobenzene units, especially liquid crystalline polymers, have attracted much interest for isomerization-induced holographic information storage because these polymer films with photochromic units exhibit a very distinct optical anisotropy after irradiation with linearly polarized light [12–17], As described by Berg et al. [14] ''when irradiated in a certain wavelength range the azobenzene undergoes random reorientation through a number of *trans–cis–trans* isomerization cycles, a stationary orientation is obtained when the optical transition moment which lies approximately parallel to the long axis of the trans azobenzene, and the azo unit is oriented in the plane perpendicular to the polarization direction of the laser beam, this anisotropic alignment of azobenzenes which leads to a local modulation of the refractive index forms the basis of the strong process''. Generally speaking, after the incident laser beam is shut off, this alignment could be permanently frozen and permanent storage is presumed to result if the glass

* Corresponding author: Yingying Zhao, Department of Chemistry, Jilin University, Changchun 130023, People's Republic of China. Fax: + 86-431-8949334; e-mail: tjli@mail.jlu.edu.cn

0032-3861/99/$ - see front matter
PII: S0032-3861(98)00595-3

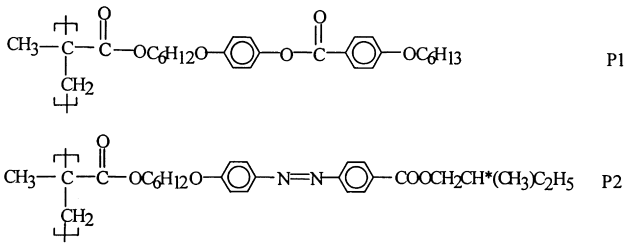

Fig. 1. The structures of the polymers P1 and P2.

transition temperature of the polymer is high. Indeed many amorphous polymers with high glass transition temperatures (higher than 100°C) have been made to increase the lifetime of the stored information [12,14]. On the other hand, recently Holme et al. [18,19] realized 10 000 optical, write, read and erase cycles in an azobenzene side-chain liquid crystalline polyester with a rather low glass transition temperature (close to room temperature), and for more than four years they have had holographically recorded thin-film grating of these polyesters without any sign of degradation. In this paper, we prepared a series of copolymers as shown in Fig. 1 with low glass transition temperatures and studied their liquid crystalline behavior, photoisomerization properties and photoinduced anisotropy at different temperatures. The results showed that these copolymers could not only show mesophases but also exhibit good photoinduced anisotropies both in the glass states and in the mesophases. The preliminary results also showed that the photoinduced anisotropy of a copolymer with 90% of azo unit did not show any decay at room temperature, it is expected to have good long-term optical storage properties, further investigation is in progress.

2. Experimental

2.1. Monomer synthesis

The solvents and materials used for synthesis are commercial products which are purified by distillation or recrystallization before use. The *S*-(−)-2-methyl-1-butanol (Aldrich 99%) was used without any further purification.

1. 4-Hexyloxybenzoic acid was prepared according to a known procedure [20], and was purified by recrystallization from glacial acetic acid. Cr 108°C, N 153°C I.
2. 4-Hydroxyphenyl-4′-hexyloxybenzoate was obtained by reaction of hydroquinone with 4-hexyloxybenzoyl chloride and recrystallized twice from ethanol–water. Mp 114–115°C. (mp 113.4°C) [21].
3. 4-(6-Bromohexyloxy)phenyl-4′-hexyloxybenzoate. This compound was prepared by the reaction of 1,6-dibromohexane with 4-hydroxyphenyl-4′-hexyloxybenzoate in acetone and recrystallized from hexane. Yield 54.4%. Cr 56.7°C (81.35 J g^{-1}) N 82.8°C (2.33 J g^{-1})I.
4. 4-[6-(Methacryloyloxy) hexyloxy] phenyl-4′-hexyloxy benzoate (M1). The monomer was synthesized by the reaction of 4-(6-bromohexyloxy)phenyl-4′-hexyloxybenzoate with potassium methacrylate in dry DMF at 60–65°C for 6 h, then recrystallized three times from hexane. Yield 72.8%. Cr 38°C, N 60°C (Cr 38°C, N 58.5°C I) [21].
5. 4-(*S*-2-methylbutyloxycarbonyl)nitrobenzene. This compound was prepared by the reaction of 4-nitrobenzoyl chloride and *S*-2-methylbutanol according to a general method and purified by column chromatography using CH_2Cl_2 as eluent. A yellow oil was obtained. Yield 80%. IR: 1729 cm^{-1} (CO ester), 1530 cm^{-1} ($-NO_2$). $[\alpha]_D^{19} = +6.1$ ($c = 1.06$, $CHCl_3$).
6. 4-(*S*-2-methylbutyloxycarbonyl)aminobenzene. The compound was prepared by the reduction of 4-(*S*-2-methylbutyloxycarbonyl)nitrobenzene with $SnCl_2 \cdot 2H_2O$ in ethanol and purified by column chromatography using CH_2Cl_2 as eluent. White solid was obtained. Yield 65%. mp: 42–44°C (43.3–45°C) [22]. IR 1693 cm^{-1} (–CO–) 1637 cm^{-1} (NH_2). $[\alpha]_D^{16} = +6.4$ ($c = 2.64$, $CHCl_3$).
7. 4-Hydroxy-4′-(*S*-2-methylbutyloxycarbonyl)azobenzene. The azo compound was synthesized according to the standard procedure [22] and purified by column chromatography using cyclohexane–ethyl acetate (4:1) as eluent. This gave the product as an orange solid. mp: 113–115°C (114.5–116°C) [22]. Yield 70%. IR: 1719 cm^{-1} (–CO–). $[\alpha]_D^{16} = +6.80$ ($c = 1.32$, $CHCl_3$). ^1H NMR($CDCl_3$, 400 MHz) δ: (ppm): 0.954 (t, 3H, $-CH_2\underline{CH_3}$). 0.991 (t, 3H, $CH\underline{CH_3}$). 1.309–1.905 (m,5H, CH and CH_2), 4.15–4.20 (m. 2H, OCH_2), 4.23–4.26 (m, 1H, OH), 6.98 (d, 2H, aromatic), 7.91–7.93 (dd, 4H, aromatic), 8.18 (d, 2H, aromatic).
8. 4-(6-Bromohexyloxy)-4′-(*S*-2-methylbutyloxycarbonyl)-azobenzene. 60 ml of 1,6-Dibromohexane, 18 g of potassium carbonate and 0.7 g of potassium iodide were heated to 65°C by stirring in 150 ml of acetone, a solution of 18.7 g (0.06 mol) of 4-hydroxy-4′-(*S*-2-methylbutyloxycarbonyl)azobenzene in 150 ml of acetone was added dropwise during 2 h. Then it was refluxed for 20 h. The inorganic salt was filtered and washed with acetone, the acetonic solution was evaporated off to about 120 ml, then 160 ml of ethanol was added. The precipitate was separated after cooled in ice-box and recrystallized from ethanol. An orange solid was obtained. Yield 19 g (66.6%). Cr 60°C S_A 66°CI. IR: 1724 cm^{-1}(–CO–). $[\alpha]_D^{16} = +3.55$ ($c = 1.49$, $CHCl_3$). ^1H NMR ($CDCl_3$, 400 MHz): δ: (ppm): 0.96 (t, 3H, $-CH_2\underline{CH_3}$), 1.03 (t, 3H, $CH\underline{CH_3}$), 1.31–1.93 (m, 13H, CH and CH_2), 3.44 (t, 2H, $-CH_2Br$), 4.06 (t, 2H, $O\underline{CH_2}CH_2$), 4.18–4.26 (m, 2H, $O\underline{CH_2}CH$), 7.01 (d, 2H, aromatic), 7.91 and 7.94 (dd. 4H, aromatic), 8.17 (d, 2H, aromatic).
9. 4-[6-(Methacryloyloxy)hexyloxy]-4′-(*S*-2-methyl-1-butyloxycarbonyl)azobenzene (M2). 6.0 g (0.013 mol) of 4-(6-bromohexyloxy)-4′-(*S*-2-methyl-1-butyloxycarbonyl)azobenzene, 4.0 g (0.032 mol) of potassium

Table 1
The characterization of the polymers

Azo-content in mol% feed	*N* (determined)	azo (determined)	*M*n	*M*w
0	0	0	0	0
10	0.37	6.21	19168	52231
25	1.39	21.8	16924	43760
50	2.44	42.2	13461	31357
75	4.01	68.7	–	–
90	4.85	82.5	–	–
100	5.95	100	12892	19717

methacrylate and 40 ml of dry DMF were stirred at 60–65°C for 4 h. The mixture was poured into ice-water, the precipitate was filtered and dried in air, then recrystallized three times from ethanol. Yield is 5.5 g (90%). mp: 71–72°C. IR: 1726 and 1708 cm^{-1} (–CO–, ester), 1632 cm^{-1} ($CH_2 = C(CH_3)$). ^1H NMR ($CDCl_3$, 400 MHz) δ: (ppm): 0.97 (t, 3H, $CH_2\underline{CH_3}$), 1.03 (t, 3H, $CH\underline{CH_3}$), 1.35–1.90 (m, 13H, CH and CH_2), 1.95 (s, 3H, $= C(CH_3)$), 4.05 and 4.17 (t, 4H, $O\underline{CH_2}CH_2$), 4.18–4.24 (m, 2H, $O\underline{CH_2}CH$), 5.55 and 6.10 (ss, 2H, $CH_2 =$), 7.01 (d, 2H, aromatic), 7.91 and 7.94 (dd, 4H, aromatic), 8.17 (d, 2H, aromatic). $C_{28}H_{36}N_2O_5$ (Mol: 482.6) Calc: C: 69.98, H: 7.55, N: 5.83; Found: C: 70.09, H: 7.59, N:5.94.

2.2. Polymer synthesis

All of the homo- and copolymers were synthesized by free-radical polymerization according to the following procedure: 500 mg of monomer or monomer mixture and 2% mol of AIBN (based on the monomer) as initiator were dissolved in 5–7 ml of fresh distilled toluene. The mixture solution was degassed by passing nitrogen for 1 h and polymerized at 70°C for 24 h. The homopolymers and copolymers were precipitated into ethanol, redissolved in $CHCl_3$ and reprecipitated with ethanol. The purified polymers were dried in vacuo at 60–65°C for 36 h. The compositions of these polymers were determined by elemental analysis. The properties of the resulting polymers are listed in Table 1.

2.3. Characterization of the monomers and polymers

IR spectra for all of the monomers and polymers were obtained using a Nicolet 5DX-FTIR spectrometer. Elemental analysis was performed with a Perkin–Elmer 240 C microanalyser. ^1H NMR spectra were measured with a Unity 400 NMR instrument operating at 400 MHz in $CDCl_3$. The polymers were characterized by gel permeation chromatography (g.p.c.) (Millipore-Waters GPC instrument) with tetrahydrofuran as eluent.

The mesomorphic properties of the polymers were studied by differential scanning calorimetry (DSC), polarized optical microscopy and X-ray diffraction analysis.

DSC was performed with a Perkin–Elmer DSC-7 instrument with a heating/cooling rate of 10K min^{-1}, the maximum in DSC enthalpy peaks was taken as the phase

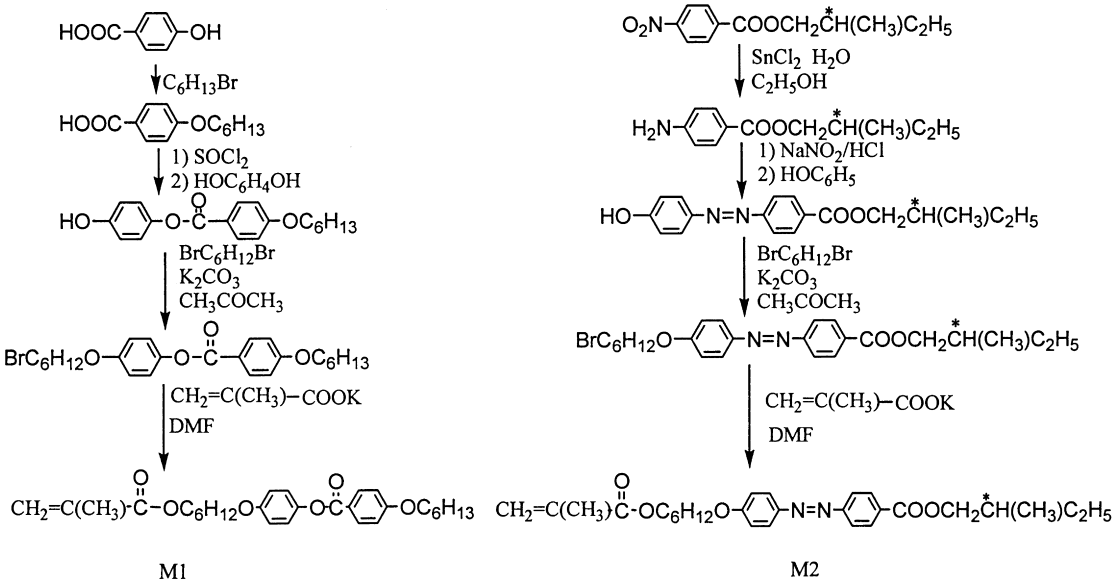

Scheme 1.

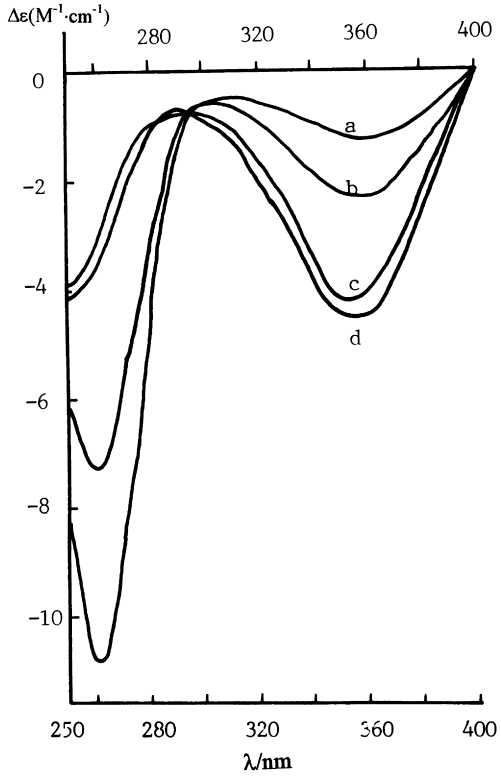

Fig. 2. The CD spectra of the copolymers.

transition temperature. The textures of the mesophases were characterized by polarizing optical microscopy with a Zeiss Jena optical microscope. The X-ray diffraction was performed with a Philip PW-1700 system with monochromatic CuKα (λ = 0.15418 nm) X-ray beam by using quenched film.

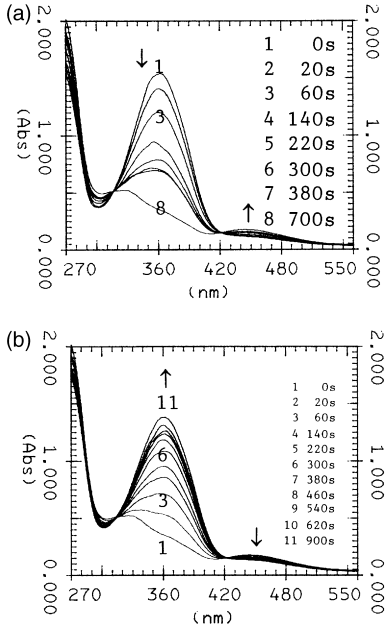

Fig. 3. UV–Vis spectral changes upon irradiation of copolymers with 50% of azo unit in $CHCl_3$. (a) irradiation at 366 nm; (b) irradiation at 450 nm. Arrows show the decrease or increase of optical density.

A solution of polymer in $CHCl_3$ was irradiated by using a 50 W Hg lamp for the photochromic investigation.

Optical activity experiments were accomplished on a WZ2-2 digital polarimeter(Shanghai, PRC) using a cell path length of 2.0 dm. Circular dichroism (CD) spectra were acquired at 25°C on a Jasco 500 A dichrograph in $CHCl_3$ solution. The same spectra regions and concentrations (100 mg l^{-1}) as for UV measurements were used.

2.4. Film preparation

Polymer films were prepared by flowing the polymer melts (120–140°C) into cells with 20 μm thickness followed by controlled cooling below the glass transition temperatures.

2.5. Experimental setup for photoinduced anisotropy

The experimental setup is analogous to the setup as described in Ref. [18]. The probe laser is an He–Ne laser at 633 nm far from the absorption band of the photochromic groups. The pumping light for inducing the anisotropy is an argon-ion laser at 514 nm with intensity of 300 mW cm^{-2}. The pumping laser beam that passed through the polymer film was split into two components using a Wallaston prism, one with polarization parallel to the polarization ($I_{\|}$) and one with polarization perpendicular to the initial polarization ($I_{\perp}$). the induced relative phase shift was calculated from the measurement of $I_{\|}$ and $I_{\perp}$ [18].

$$\Delta\phi = \sin^{-1}\sqrt{\frac{I_{\perp}}{I_{\perp} + I_{\|}}}$$

3. Results and discussion

3.1. Synthesis and characterization of monomers and polymers

The preparation of monomers M1 and M2 is summarized in Scheme 1. The polymerization was carried out in degassed toluene. The completeness of polymerization was determined by the disappearance of the methyl and vinyl proton signals of the methacryloxy group at 1.94–1.96 ppm and 5.50–6.10 ppm in the ^1H NMR spectra and the absorption at 1600–1640 cm^{-1} in the IR spectra.

The polymer composition was determined by elemental analysis (N value), acceptable yields (58–83%) and agreement between initial comonomer ratio and copolymer composition could be reached (see Table 1).

No reliable measurements of optical rotatory power on azobenzene-containing monomers and polymers could be obtained due to their high absorption, but their chirality can be identified from CD spectra as shown in Fig. 2. The CD spectra in $CHCl_3$ solution show that all of the

Table 2
DSC data for the polymers

Azo-content (/%)	Phase transition (/°C)
0	G 17, Sc 73.7, S_A 127.7 I
10	G 14, Sc* 85.8, S_A 123.0 I
25	Sc* 111.4, S_A116.0 I
50	Sc*? 119.4 I
75	Sc*? 100.3 I
90	G48.7, Sc* 83.2, S_A 96.9 I
100	G49.0, Sc* 61.9, S_A 98.1 I

copolymers containing azo groups exhibit a broad negative band connected to the $\pi-\pi^*$ electronic transition which is centered around 360 nm in close correspondence with UV absorption pattern (one of which is shown in Fig. 3). All of the CD spectra were taken by the same concentration (100 mg l^{-1}), from these CD spectra, we can also see that along with the increasing concentration of chiral composition the ellipticity in the $\pi-\pi^*$ transition spectral regions also increased.

3.2. Photoisomerization of polymers

We also investigated the photoisomerization of the copolymers by using UV light at 366 nm and visible light at 450 nm. For example, Fig. 3 shows the photoisomerization of the polymer containing 50% of azo group (feed content) in $CHCl_3$ solution. The irradiation of solution of $CHCl_3$ with UV light at 366 nm leads to *Z–E* isomerization without any side reactions. This is proved by the existence of isobestic points at 317 nm and 422 nm in the corresponding UV–Vis spectra [23] (Fig. 3a). The reversibility of the *E–Z* isomerization was proved by irradiation at 450 nm, this shows an increase in the absorbance at 350–360 nm up to ca. 88% of the original value (Fig. 3b).

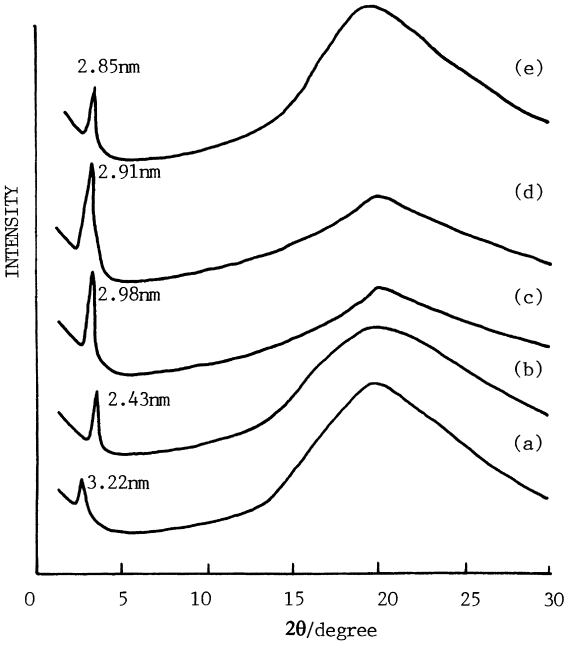

Fig. 4. The X-ray diffractograms of some polymers. (a) and (b) the quenched films of homopolymer P2 after annealing at 80°C and 54°C respectively; (c) and (d) the quenched films of copolymers with 90% of azo unit after annealing at 88°C and 73°C, respectively, (e) the quenched film of copolymer containing 50% of azo unit.

3.3. Liquid crystalline behavior

All of the polymers exhibited mesophase behavior. The phase transition temperatures recorded by DSC are given in Table 2 in detail. For the homopolymer P1, a smectic A and a smectic C phase could be observed by polarized optical microscopy with fan shaped texture, the phase transition temperatures (g 17°C, Sc 73.7°C, S_A 127.7°C I) of this polymer are slightly different from those reported in the literature (g 16°C, Sc 85°C, S_A 128°C I) [21]. For the chiral copolymers containing 10% and 25% of the chiral azo group, focal-conic fan shaped texture could also be seen by polarized optical microscopy, combining with the results of DSC, these two copolymers exhibited S_A phases and Sc* phases. But for the polymers containing more than 25% of the azobenzene units, no typical textures could be seen under the microscope, so X-ray investigation were carried out. Fig. 4 shows the X-ray diffractograms obtained from the films of P2 (curves a and b) and copolymers containing 90% (curves c and d) and 50% (curve e) of azo groups respectively. All of the X-ray diffractograms reveal a sharp first diffraction peak at low angles which is associated with smectic layers and a broad reflection at wide angles which is associated with the lateral packing. From this figure we can see that the values of these first diffraction peaks (2.4–3.2 nm) are generally in accordance with or shorter than the molecular lengths with all transformations (for P1, L = 3.0 nm; for P2, L = 3.2 nm), so all of the smectic phases are in the monolayer arrangmental style. From curve a we can see that the first diffraction peak of P2 is equal to its molecular length, so the molecular arrangemental style should be monolayer S_A. From curve b we can see that the first diffraction peak of P2 is greatly shorter than its molecular length, according to the equation: $d = L.\cos\theta$ (for this polymer L = 3.22 nm, d = 2.43 nm), the tilt angle of this smectic phase is 41°, so this tilted smectic phase should be Sc* phase. Combining the results of DSC, polarizing optical microscopy and X-ray diffraction studies resulted in Fig. 5, which shows the phase diagram of this series of polymers in detail.

3.4. The photoinduced anisotropy at room temperature

The photoinduced anisotropy or birefringence is of greater interest from a holographic point of view, particularly for wavelengths outside the optical transmission, since it leads to higher recording efficiency. We investigated their photoanisotropy at 633 nm under the action of pumping light at 514 nm. A typical experimental result of the induced anisotropy in a sample with 90% of azo unit (feed content) is

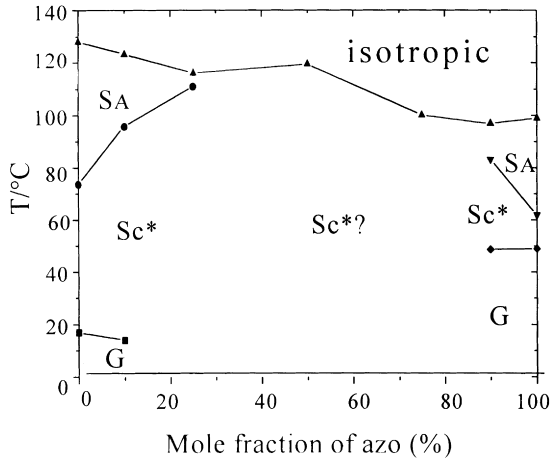

Fig. 5. The phase diagram of these polymers.

shown in Fig. 6. At point a linearly polarized pumping light (514 nm) is turned on; at point b, the pumping light is turned off; at point c, circularly polarized light (514 nm) is turned on for erasing the induced anisotropy.

From the UV–Vis spectra as shown in Fig. 3, we can see that the maximum absorption band of azobenzene chromophore is 365 nm which is the $\pi-\pi^*$ absorption band connected with the stable ground state (i.e. the *trans* state) of the chromophore, the weak absorption band centered at 450 nm is the $n-\pi^*$ absorption band related to the *cis* state of the azochromophore. Thus irradiation at 366 nm causes a *trans–cis* isomerization whereas irradiation at 514 nm causes a *trans–cis–trans* isomerization cycle [19]. So after repeating *trans–cis–trans* isomerization under this plane laser (514 nm), a stationary orientation is obtained. This can be seen in Fig. 6 from point a to point b. At point b the laser light is turned off, while for this copolymer the photoinduced anisotropy does not show any decay as shown in Fig. 6. Actually the photoinduced anisotropy still

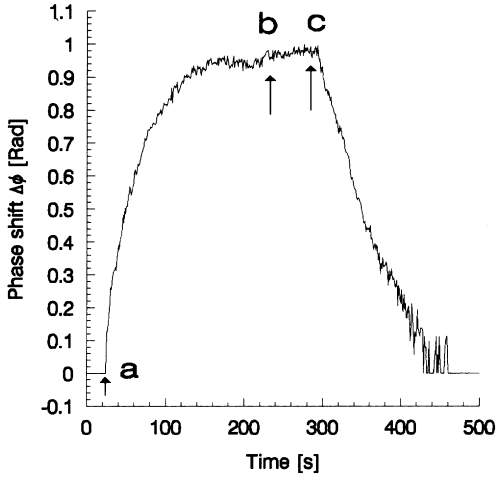

Fig. 6. A typical cycle of the photoinduced anisotropy of a copolymer with 90% of azo unit. At point a, linearly polarized pumping light (514 nm) is turned on; at point b, the pumping light is turned off; at point c, circularly polarized light (514 nm) is turned on to erase the induced anisotropy.

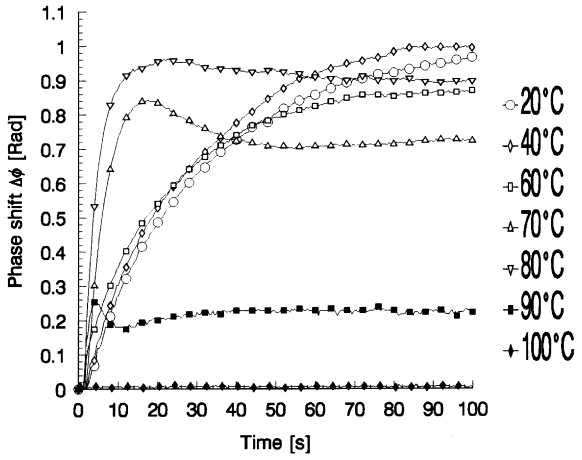

Fig. 7. The temporal behavior of the photoinduced anisotropy of the copolymer with 90% of azo unit (its phase transition is g 48.7, Sc* 83.2, S_A 96.9 I as shown in Table 2).

does not decay in several days. This result implies that the copolymer has potential application in long-term optical storage. Further investigation is in progress. At point c, a circularly polarized beam was switched on, the photoinduced anisotropy decreased rapidly, resulting in loss of about 99% of the anisotropy. The photoanisotropy can be rewritten and erased many times at room temperature.

3.5. Temporal behavior of induced anisotropy

We investigated the temporal behavior of photoinduced anisotropy of the copolymer with 90% of azo unit (feed content) with the pumping laser intensity of 300 mW cm^{-2}. The typical temporal behavior of induced anisotropy as a function of film temperature is shown in Fig. 7. From Fig. 7, it can be seen that the maximum anisotropy is induced at 40°C which is very near the glass transition temperature of this polymer (Tg = 48.7°C). Between 40°C and 80°C, the value of the photoinduced anisotropy fluctuated randomly with no clear trend. With increasing temperatures above 70°C, the anisotropy decreased rapidly and became zero, with experimental uncertainty above 100°C. Referring to Table 2, we can see that the photoinduced anisotropy is not removed when the temperature is in the mesophase range, but the photoinduced anisotropy shows fluctuations. An analogous phenomenon was reported in Ref. [19]. The reason is not yet fully understood, but it is apparent that the induced anisotropy could be stored in aggregated phases such as smectic phases as shown in our result.

4. Conclusion

So in summary, in this paper we have described the preparation and investigation of a series of liquid crystalline copolymers with azo groups, the results showed these polymers have wide mesophase temperature ranges and good

photoactivity. And our results also showed that the linearly polarized laser beam can orient these chromophores in the side-chain polymers not only in the glass states below *T*g but also in the mesophase between *T*g and *T*i. The photoinduced anisotropy can be erased not only by using circularly polarized light but also by controlling temperatures greater than their isotropic transitions. And because the photoinduced anisotropy of the copolymers with 90% and 100% of azo units did not show any decay at room temperature, they are expected to have good long term optical storage properties, further investigation is in progress.

References

[1] Birenheide R, Eich M, Jungbauer DA, Herrmann-Schonherr O, Stoll K, Wendorff JH. Mol Cryst Liq Cryst 1989;177:13.
[2] Attard G, Willams G. Nature 1989;326:544.
[3] Nakamura T, Ueno T, Tani C. Mol Cryst Liq Cryst 1989;169:167.
[4] Wiesner U, Reynolds N, Boeffel C, Spiess HW. Liq Cryst 1992;11:251.
[5] Muller M, Zentel R. Makromol Chem 1993;194:101.
[6] Eich M, Wendorff JH, Reck B. Makromol Chem Rapid Commun 1987;8:59.
[7] Ikeda T, Miyamoto T, Sasaki T, Kurihara S, Tazuke S. Mol Cryst Liq Cryst 1990;188:235.
[8] Scherowsky G, Beer A, Coles HJ. Liq Cryst 1991;10:809.
[9] Ringsdorf H, Urban C, Knoll W, Sawodny M. Makromol Chem 1992;193:1235.
[10] Niesel FT, Springer J, Czapla S, Wolff D, Rubner J. Makromol Rapid Commun 1994;15:7.
[11] Niesel FT, Rubner J, Springer J. Makromol Chem Phys 1995;196:4103.
[12] Natansohn A, Rochon P, Barrett C, Hay A. Chem Mater 1995;7:1612.
[13] Rochon P, Gosselin J, Natansohn A, Xie S. Appl Phys Letter 1992;60:4.
[14] Berg Rolf H, Hvilsted S, Ramanujam PS. Nature 1996;383:506.
[15] Eisenback CD. Mackromol Chem 1978;179:2489.
[16] Eich M, Wendorff JH. Makromol Chem Rapid Commun 1987;8:469.
[17] Eich M, Wendorff JH, Reck B, Ringsdorff H. Makromol Chem Rapid Commun 1987;8:59.
[18] Holme NCR, Hvilsted S, Ramanujam PS. Applied Optics 1996;35:4622.
[19] Holme NCR, Hvilsted S, Ramanujam PS. Optical Letters 1996;21:1902.
[20] Jones B. J Chem Soc 1935:1874.
[21] Roderich G, Rubner J, Zschuppe V, Wolff D, Springer J. Makrom Chem 1993;194:1125.
[22] Newton J, Walton H, Coles H, Hodge P. Mol Cryst Liq Cryst 1995;260:107.
[23] Nieman M, Ritter H. Makromol Chem 1993;194:1169.